

Targeting STAT3 abrogates Tim-3 upregulation of adaptive resistance to PD-1 blockade on regulatory T cells of melanoma

Lili Huang

Tongji University Tenth People's Hospital: Shanghai Tenth People's Hospital

Yu Xu

Fudan University Shanghai Cancer Center

Juemin Fang

Tongji University Tenth People's Hospital: Shanghai Tenth People's Hospital

Weixing Liu

Tongji University Tenth People's Hospital: Shanghai Tenth People's Hospital

Jianhua Chen

Tongji University Tenth People's Hospital: Shanghai Tenth People's Hospital

Zhuqing Liu (✉ zhuqingliu2013@163.com)

Tongji University Tenth People's Hospital: Shanghai Tenth People's Hospital

Qing Xu

Tongji University Tenth People's Hospital: Shanghai Tenth People's Hospital

Research

Keywords: Regulatory T cells, Tim-3, Melanoma, Anti-PD-1 therapy, STAT3

Posted Date: October 1st, 2020

DOI: <https://doi.org/10.21203/rs.3.rs-83300/v1>

License: © ⓘ This work is licensed under a Creative Commons Attribution 4.0 International License.

[Read Full License](#)

Abstract

Background

Programmed cell death-1 (PD-1) blockade immunotherapies have demonstrated excellent clinical benefits in multiple cancers, but < 20% of melanoma patients respond to these treatments. Thus, it is crucial to understand for getting awareness of the dynamic changes vibrant transformations in the tumor microenvironment (TME) after PD-1 blockade, in exploring novel intervention targets as a potential therapy, for developing immunotherapy efficacy.

Methods

To ascertain the differentially expressed between PDCD1^{low} and PDCD1^{high} subsets and further PDCD1 related genes in skin cutaneous melanoma (SKCM) patients, a genomic analysis was conducted by The Cancer Genome Atlas (TCGA) datasets and web platform TIMER2.0 datasets. Pathway enrichment analysis was performed using the Kyoto Encyclopedia of Genes and Genomes (KEGG) pathway. Peripheral blood mononuclear cells (PBMCs), regulatory T (Treg) cells and B16F10 melanoma mouse were used as models. The cellular and molecular characteristics and mechanisms of Treg cells in melanoma were assessed by performing gene expression studies, immunohistochemistry, RNA sequencing, and flow cytometry.

Results

Here, we evaluate the countenance of T cell immunoglobulin and mucin-domain containing-3 (Tim-3), various immunosuppressive factors within tumor infiltrated regulatory T (Treg) cells after treated with anti-PD-1 or the indicator transduction and activator of transcription 3 (STAT3) inhibitors. Tim-3 gene is expressed differentially between PD-1^{low} and PD-1^{high} subsets from TCGA datasets and melanoma patients' biopsies. Increased expression of Tim-3 is markedly observed within the tissues of the PD-1 blockade resistance of melanoma patients. Targeting STAT3 significantly boosts the response of resistant-PD-1 therapy within the melanoma mouse model. Mechanistically, the manifestation of STAT3 decreases the expression of Tim-3 and various cytokines in the purified Treg cells from individual peripheral blood mononuclear cells (PBMCs) and murine melanoma model, limiting the immunosuppression of Treg cells.

Conclusions

Our findings indicate that Tim-3 expression on Treg cells within the TME is STAT3-dependent, providing support to STAT3 as a target and enhancing the immunotherapy for patients suffering from melanoma.

Background

Recently, designed cell death-1 (PD-1) blocking antibodies, produce excellent effects concerning the medication of numerous tumors, containing melanoma, non-small-cell lung cell cancer, and bladder

cancer [1–3]. However, patients who receive nivolumab show low responses [4, 5]. Thus, it is essential to comprehend the vibrant alterations of adaptive resistance within the tumor microenvironment (TME) after PD-1 blockade and explores novel intervention targets as a possible therapy for improving the efficacy of immunotherapy.

With the development in the study of the TME, innovative, and synergistic combination therapies perform excellent efficacy in melanoma. While blocking one more immunomodulatory pathway is still needed to explore in eradicating the advanced melanomas [6]. One prominent strategy is blocking dual immune harrier receptors in T cells by targeting both the inhibitory T cell immunoglobulin and mucin-domain containing-3 (Tim-3) and PD-1[7]. Tim-3 is considered the checkpoint receptor mediating T cell tiredness in the immune microenvironment [8, 9]. And Tim-3 also presents a crucial event in the immunosuppression of CD8⁺ T cells, whereas regulating monitoring T (Treg) cells enhances the function of effector [10, 11]. Tumor-associated Treg cells which emphasized inhibitory checkpoint receptor Tim-3 comprises a particular subset of tissue Treg cells by promoting tumor progression in the mouse or human melanoma tissues by binding to galectin-9 expressed in melanoma cells [12, 13]. Moreover, methods targeting T cells via the PD-1 immune checkpoint pathway resulted in increased Tim-3 proportion [14, 15]. The previous research showed that effective anti-PD-1 treatment could decrease Tim-3 expression on Treg cells of head and neck squamous cell carcinoma (HNSCC) tumors [16]. However, the dynamic changes of Tim-3 on Treg cells in anti-PD-1 nonresponse melanoma patients, potential cross-talk of PD-1 and Tim-3 in tumor-infiltrating lymphocytes (TILs), and the mechanism of the regulation of the two checkpoint receptors above have not been elucidated.

Indicator transduction and activator of transcription 3 (STAT3) are constitutively mediate tumor proliferation, progression and metastasis, and immunity in the TME [17, 18]. STAT3 activation in adaptive immune cells results in inhibiting immune regulation and immunosuppressive factors secretion [19]. Moreover, STAT3 acts as a co-transcription pathway for forehead box P3 (Foxp3) and a mediator for other STAT3-associated targets, including interleukin-10 (IL-10), in Treg cells [20]. Furthermore, STAT3 has been identified as in promoting the articulation of Foxp3 within CD4⁺CD25⁺ Treg cells in TME, enhancing immune suppressive function [21, 22]. A STAT3 inhibitor WP1066 could perform an excellent antitumor response due to inhibiting the proliferation of Treg cells [23]. Furthermore, STAT3 can directly control the promotor of converting development component in Treg cells of T cell-precise SOCS3-inadequate mice [24]. As to whether and how the STAT3 pathway regulates the inhibitory checkpoint receptor Tim-3 in the TME is still anonymous.

In this study, we observed that higher expression of Tim-3 on Treg cells is associated with the resistance of melanoma patients treated with anti-PD-1. Moreover, using Stattic to target the STAT3 pathway, we observed that Tim-3 downregulation *in vitro* phenotype and function assays and an *in vivo* melanoma model. Interestingly, depletion STAT3 in the preclinical model damped the tumor growth and Treg cells recruitments and increased the CD8⁺/CD4⁺ ratio in melanoma. Furthermore, synergistic combination therapies with Stattic impairs the responses to anti-PD-1 melanoma. Our findings reveal that combing STAT3 downregulation and anti-PD-1 is presented as a potential medicinal target for diseased persons.

Materials And Methods

The Cancer Genome Atlas (TCGA) analysis

The melanoma dataset had been transferred from the TCGA program using cBioportal for Cancer Genomics (www.cbioportal.org). The gene expression of PDCD1, HACVR2, and STAT3 had been evaluated using Spearman's rank correlation coefficient using the publically available TCGA dataset. The patients' clinical information along with the mRNA expression data (RNA Seq V2 RSEM) were acquired from cBioportal for Cancer Genomics (www.cbioportal.org). The association between immune infiltrates and genetic and clinical features were estimated by the web platform TIMER2.0 datasets (<http://timer.cistrome.org/>). Kaplan-Meier curve analysis and log-rank tests were performed to observe the survival rate of melanoma patients using web platform TIMER2.0 datasets (<http://timer.cistrome.org/>).

Correlation and pathway enrichment analysis

The gene expression of PDCD1, HACVR2, and tumor infiltrated Treg cells was performed in primary and metastasis melanoma using the *t-test*. Patients from TCGA were divided into two quartiles according to the expression of PDCD1 stated in a divergent way. Genes had been discovered corresponding to the criteria of $p < 0.05$, the fold change > 1.5 . The top significantly differentially expressed genes were determined in the PD-1 high representation and PD-1 low representation groups by the p values ($n=472$). To cluster these genes in the pathway of melanoma, we uploaded the related genes on the Database for Annotation, Visualization and Integrated Discovery (DAVID) functional annotation analysis website (<https://david.ncifcrf.gov/>). We selected the top 30 pathways in the Kyoto Encyclopedia of Genes and Genomes (KEGG) pathways analysis.

Reagents

The anti-human PD-1 antibody (used at 10 $\mu\text{g}/\text{mL}$ concentration) was obtained from Merck & Co., Inc. (New Jersey, USA). In VivoM Ab anti-mouse PD-1 (used at 10 $\mu\text{g}/\text{mL}$ concentration) and In VivoM Ab anti-mouse IgG2a was purchased from Bioxcell (New Hampshire, USA). STAT3 inhibitor Stattic (used at 5 μM concentration) was purchased from MedChemExpress (New Jersey, USA). Stattic was dissolved in DMSO. Recombinant human IL-2 (used at 200 IU/mL concentration) was obtained from Thermo Fisher Scientific (Waltham, USA) and solubilized in PBS with 1% BSA. Ultra-LEAFTM Purified anti-human CD3 antibody (used at 1 $\mu\text{g}/\text{mL}$ concentration, clone: OKT3), Ultra-LEAFTM Purified anti-human CD28 antibody (1 $\mu\text{g}/\text{mL}$ concentration, clone: 28.2) and cell activation cocktail (with Brefeldin A) were purchased from Biolegend (San Diego, USA). Fixable viability Dye eFluorTM 780 was obtained from Thermo Fisher Scientific (Waltham, USA) and solubilized in DMSO.

Cell Culture

Melanoma cell lines B16-F10 were purchased from the American Type Culture Collection (ATCC). Cells had been refined at 37 °C with 5% CO₂ and preserved within Dulbecco's Modified Eagle Medium (DMEM)

(Gibco, USA) with 10% fetal bovine serum (FBS) (Gibco, USA), and 1% penicillin/streptomycin (Gibco, USA). Peripheral blood mononuclear cells (PBMCs) and purified Treg cells were cultured in 1640 mediums (10% FBS) with 1% penicillin/streptomycin after coated-plate with anti-CD3, anti-CD28, and IL-2.

Patients and samples

Human specimens had been achieved with the approval of Tongji University. Blood samples have been taken from healthy donors, centrifugated (2000 rpm for 20 min at 4 °C), and accumulated for flow cytometry analysis. Tissue samples were obtained and isolated from melanoma patients for flow cytometry and immunohistochemistry (IHC) staining. RNA extracted from melanoma tissue was used for RNA sequencing and data analysis.

RNA sequencing and data analysis

Fresh tumor tissues of melanoma patients were acquired by isolating the sections of metastases from patients without anti-PD-1 therapy. The medical and pathological features of the melanoma persons in this study have been shown in Table 1. RNA sequencing (RNA-seq) was performed on fresh frozen tumor tissues (n=6). The analysis of RNA-seq data was performed using a two-pass method with STAR. The readings mapped to each gene were enumerated using RSEM, and expression level reading counts were normalized using the FPKM method. Genes stated in a divergent way had been categorized according to standards of $p < 0.05$ and a fold variation > 2.0 . The top significantly differentially expressed conveyed genes had been determined in the PD-1 high representation and PD-1 low representation groups by the p values.

Lymphocyte Isolation

For getting single-cell suspension samples for flow cytometry analysis, tissues were isolated from melanoma patients into small pieces. Then, the small pieces were made into tumor suspensions processed by the way a 70 μ m cell filter and centrifuged for 20 min at 2000 rpm at 4 °C using Ficoll-Paque Plus. After centrifugation, the tumor-infiltrating lymphocytes were transferred into a new tube and washed with RPMI-1640 medium including 10% FBS twice. Lysis buffer (BD biosciences, USA) was utilized to remove the red cells when needed. Peripheral blood mononuclear cells (PBMCs) and TILs of mice had been quarantined following the same protocols. PBMCs and melanoma TILs were incubated in 1640 medium and TCR stimulation with anti-CD3, soluble anti-CD28, and IL-2 for three days. For had been quarantined of PD-1 blockade and STAT3 inhibition on Treg cells *in vitro*, we classified Treg cells from PBMCs of healthy donors by flow sorting centered upon CD4⁺CD25⁺CD127⁻ staining cells. Then, Treg cells were cultured in 1640 mediums (10% FBS) with 1% penicillin/streptomycin later coated-plate with anti-CD3, anti-CD28, and IL-2. IgG, anti-PD-1 (10 μ g/mL, Merck, USA), or Stattic (5 μ M, MCE, USA) treatments were added as indicated for 48 hours.

Flow cytometry

Single-cell suspensions were incubated in staining buffer. All antibodies gained after BD bioscience, Biolegend, eBioscience, or R&D system. Surface staining was performed in staining buffer for 30 min at 4 °C in the dark. Before stream cytometry, PBMCs and TIL need to stimulate with 0.25 mg brefeldin A or four hours at 37 °C. PBMCs and TILs for extracellular staining were stained with CD4, CD25, CD127, PD-1, and Tim-3. Fixable viability Dye eFluor™ 780 had been exploited in eliminating dead cells. For intracellular staining, cells had been first static/permeabilized with a record component staining buffer set for 60 min. Besides, Single-cell suspensions subjected to intracellular antibody staining for Foxp3, Granzyme B, IL-10, IL-17A, and TGF-β. All samples were incubated in a staining buffer and stored in the dark. Data were collected with a Fortessa or Cantoll flow cytometer (BD bioscience, USA) and evaluated applying FlowJo version 10 (FlowJo LLC, USA).

Mouse model

All experiments for animals had been executed corresponding to the procedures and under the recommendations endorsed from the institutional Animal Care and Use Committee of Tongji University. C57BL/6 mice aged six weeks had been in the experimental group. B16-F10 cells (5×10^5 cells) were subcutaneously injected into the limbs of immunocompetent C57BL/6 mice. Tumors were measured using a digital caliper, and their volume was calculated with the formula $(width)^2 \times length / 2$. The weight of the mice was also calculated every two days. After incubation for six days, the mice were subjected to IgG2a as control, anti-PD-1, STAT3 pathway inhibitor Stattic, and combination anti-PD-1 with Stattic treatments. The mice were euthanized, tumors, spleens, and other systemic organs were dissected at the end-point experimental analyses. Tumors and spleens were used to prepare single-cell suspensions for flow cytometry analysis. The main systemic organs were fixed with paraformaldehyde at 4 °C for hematoxylin and eosin (H&E) and Terminal deoxynucleotidyl transferase-mediated dUTP-biotin nick end labeling assay (TUNEL) discoloration. Mice had been randomly assigned for treatment groups.

Immunohistochemistry staining

Tissue samples from humans and animals were fixed with paraformaldehyde and embedded with paraffin, then cut into 5 mm sections for further staining. For immunohistochemistry staining, sections were deparaffinized with xylene and rehydrated. Antigen retrieval was performed with a heated antigen unmasking solution (1.0 mM EDTA, 0.05% Tween 20, pH 8.0). Primary antigens Tim-3 (1:1000 for IHC, Cell Signalling Technology, USA) was incubated on the slices overnight at 4 °C after 1 hour of serum blocking. The DAB chromogen was used for IHC, followed by counterstaining with hematoxylin QS. On the second day, the sections were exposed to the corresponding secondary antibodies for 1 hour at room temperature. Slides were digitally scanned using NanoZoomer S210 (Hamamatsu, Hamamatsu, Japan) with a 20X objective, and automated image analysis was performed using NOPview2 software. The comparative expression of Tim-3 was finalized employing ImageJ software within normal (n=3) and melanoma (n=3) tissues.

Statistical analysis

Statistical analyses had been presented utilizing GraphPad Prism v.8.0 (San Diego, USA). Data points were shown as the mean \pm SEM of biological replication. Implication is indicated as * $p < 0.05$ or ** $p < 0.01$ or *** $p < 0.001$ for the total legends. Two-tailed combined or unmatched Student's-tests had been achieved for the discovery of significant differences in normally distributed data. For multiple group comparisons, one- or two-way ANOVA with multiple comparison correction had been utilized for defining disagreements. Correlations were determined with Pearson's coefficient.

Results

Expression levels of HAVCR2 and PDCD1 are correlated on Treg cells in advanced melanoma

Analysis from the TCGA database demonstrated that the genes HAVCR2 encoding Tim-3 was enriched in differentially expressed genes between PD-1^{low} and PD-1^{high} cohorts (Figure 1A). To evaluate whether HAVCR2 expression was associated with PD-1 expression in melanoma, we performed mRNA expression of PDCD1 encoding PD-1 and HAVCR2 in tumor biopsies and TCGA databases. Correlation results demonstrated that HAVCR2 showed positive interaction with PDCD1 in the TME (Figure 1B-C). Exploring the clinical significance of PDCD1 and HAVCR2 in melanoma patients, we analyzed the gene expression levels in primary and metastasis melanoma. Expectedly, both PDCD1 and HAVCR2 expression were significantly higher in advanced melanoma compared to primary melanoma in TCGA datasets (Figure 1D-E). Otherwise, we also found that tumor infiltrated Treg cells were increased in metastasis melanoma (Figure 1F). To investigate the dynamic changes of PDCD1 and HAVCR2 on Treg cells in the tumor progression, we analyzed the gene expression on tumor infiltrated Treg cells in TCGA datasets. Interestingly, the checkpoint molecules PDCD1 and HAVCR2 were upregulated in advanced melanoma patients (Figure 1H-I). Further corroborating these observations, a positive correlation > 0.4 between Tim-3 and PD-1 expression on human Treg cells was discovered (Figure 1G). Overall, these data suggested that Tim-3 is engaged by PD-1 on Treg cells toward the progression of melanoma.

Tim-3 is upregulated Treg cells upon anti-PD-1 treatment

Although PD-1-blocking antibodies have presented excellent effects in melanoma therapy, only a few patients experience ideal therapeutic effects [4, 5]. To elucidate the role of immune cells after anti-PD-1 therapy, we assessed the proportion changes of Treg cells in the PBMCs. Results showed a dramatic rise in Treg cell expression, which reflecting immune regulation changes after checkpoint blockade therapy (Figure 2A-B). To further identify functional differences of Treg cells, we then investigate the expression of Tim-3 on CD4⁺CD25⁺Foxp3⁺ Treg cells from PBMCs or purified Treg cells upon anti-PD-1 antibody. The dynamic expression of Tim-3 on Treg cells was checked for confirming the immune suppression after incubated with an anti-PD-1 antibody in the standard medium for 48 h. As shown in Figure 2C, the percentage of Tim-3⁺ cells were significantly upregulated in Treg cells after PD-1 blockade ($p < 0.01$). We also found that immune-suppressive cytokines production IL-10 and TGF- β were highly increased in Treg cells after anti-PD-1 treatment (Figure 2 D-E; $p < 0.05$). Besides, purified Treg cells from PBMCs were further sorted to understand the characteristics of Tim-3 expression on Treg cells completely. Similarly,

flow cytometric data demonstrated that blockade PD-1 pathway markedly increased the level of Tim-3 expression on purified Treg cells, suggesting an upregulated immune suppression (Figure 2F, $p < 0.001$). Further corroborating these observations, the cytokines production IL-10 on purified Treg cells were significantly increased after anti-PD-1 treatment (Figure 2G, $p < 0.01$). Moreover, melanoma samples from patients were obtained and analyzed to investigate the levels of Tim-3 and immunosuppressive factors. In melanoma tissues, we found a significant upregulation of Tim-3 on Treg cells after anti-PD-1 therapy *in vitro* (Figure 2H, $p < 0.05$), which was similar to PBMCs. Thus, these findings suggest that blocking the PD-1 pathway significantly upregulates Tim-3 expression on Treg cells. Consistent with our previous study, we also found that Tim-3 downregulated with decreasing the proportion of TGF- β secretion after PD-1 pathway blockade both in PBMCs and melanoma tissues, reflecting the excellent efficacy of anti-PD-1 therapy (Figure S1A-D). These results support the hypothesis that Tim-3 expression can be a potential biomarker for predicting tumor-progression and resistance to anti-PD-1 immunotherapy in melanoma patients.

For verification, that Treg cells were in a functional state, the proliferation of Treg cells had been analyzed after different treatments. It was hoped that Treg cells in the anti-PD-1 group displayed a lower proliferation than did those in the control group (Figure S2A-B), which suggested a suppressive state of Treg cells after anti-PD-1 therapy. Brought jointly, these results confirmed that Tim-3 expression represents an adaptive response for keeping the suppressive status of Treg cells in response to PD-1 blockade.

To confirm that the upregulation of the Tim-3 level after anti-PD-1 immunotherapy, we analyzed the immunohistochemistry (IHC) staining using samples from anti-PD-1 nonresponding melanoma patients. As expected, the checkpoint molecules Tim-3 was increased upon PD-1 immunotherapy in advanced melanoma patients (Figure 3A-B). These results were corroborated with the aforementioned data. To identify the role of Tim-3 expression on tumor growth, we established an immunocompetent skin melanoma model using B16-F10 cells. Our data identified that the PD-1 pathway blockade upregulated the proportion of Tim-3 expression on melanoma-associated Treg cells (Figure 3C). Moreover, we observed a slight rise in the secretion of IL-10 and TGF- β with anti-PD-1 therapy *in vivo* compared to control melanoma mice, implying an enhanced immune suppression (Figure 3D-E). These results were similar to the previous *in vitro* data. Taken together, these results confirmed that Tim-3 expression represents an adaptive response to maintain the suppressive status of Treg cells in response to PD-1 blockade.

To investigate the molecular mechanism of Tim-3 upregulation upon an anti-PD-1 treatment, we evaluated the candidate differentially expressed genes between PD-1^{low} and PD-1^{high} cohorts using the online website of DAVID. As shown in Figure 3F, the top 30 related functional and signaling pathways were identified. These genes were enriched in pathways related to cancers, PI3K-Akt signaling, cytokine-cytokine receptor interaction, Jak-STAT signaling pathway, and so on (Figure 3F). The STAT3 pathway has been identified that presented an essential role in the inflammatory response of adaptive immune cells. To determine the clinical significance of the STAT3 gene, we performed the clinical correlative

outcomes in TCGA melanoma datasets (Figure 3G). It was not unexpected for STAT3 to be strongly associated with OS in the melanoma patients (Figure 3G). Above all, these data proposed that STAT3 could mediate the tumor immunity upon PD-1 blockade.

Downregulation of STAT3 decreases Tim-3 expression on Treg cells

The STAT3 pathway performs the core part of the inflammatory response of adaptive immune cells. And STAT3 also acts both as a co-transcription pathway for Foxp3 and a mediator for IL-10 in Treg cells [19]. To further address the molecular mechanisms triggered in Treg cells upon Tim-3 upregulation, we evaluated a crucial mediator of carcinogenesis STAT3 through immunosuppression in melanoma. To identify the relationship between tumor infiltrated levels of Treg cells and STAT3, the melanoma cohort of the TCGA dataset was filtered and analyzed by Spearman correlation analysis. As shown in Figure 4 A, STAT3 showed a high correlation with Treg cells in melanoma datasets. Moreover, PDCD1 and HAVCR2 exhibited a positive correlation with STAT3, but the association in PDCD1 is weak ($r_{\text{pearson}} = 0.195; 0.381$, respectively) (Figure 4 B-C). These findings support that STAT3 could act as a crucial mediator of Treg cells associated checkpoint receptor expression in TME. Besides, we also found that the expression of the level of p-STAT3 was increased in the anti-PD-1 group with increased Tim-3 expression both *in vitro* or *in vivo* (Figure 4D-E). According to the above results, we hypothesized that Tim-3 was upregulated through the STAT3 pathway in Treg cells after the PD-1 blockade.

A small-molecule inhibitor of p-STAT3 (Stattic) was used to confirm whether Tim-3 was regulated after anti-PD-1 therapy. Cells were incubated with the inhibitor for 48 h after anti-CD3/28 stimulation. Flow analysis indicated that Stattic reduced the level of Tim-3 compared with the vehicle controls after TCR stimulation (Figure 4F). Moreover, we also performed a flow cytometric analysis of Tim-3 on Treg cells upon depletion of STAT3 in melanoma tissues (Figure 4G). Similar to the results, we also found a slight decrease in the Tim-3 expression on melanoma infiltrated Treg cells (Figure 4G), suggesting that inhibited STAT3 could abrogate the Tim-3 expression on Treg cells. However, we also found that PD-1 expression upregulated upon exposure to Stattic (Figure 4H). To determine the impact of STAT3 downregulation on Treg cells function, we used Treg cells to analyze the production of TGF- β by stimulating with brefeldin A *in vitro* (Figure 4I). The percentage of cytokines TGF- β in Treg cells was found to decrease after STAT3 depletion (Figure 4I, $p < 0.0001$). Melanoma infiltrated Treg cells exhibited similar *in vitro* Tim-3 increasing trend in STAT3 pathways blockade. These results strongly suggested that STAT-3 downregulation damped the level of Tim-3 expression in Treg cells, leading a decreased immunosuppression. Furthermore, to confirm the therapeutic efficacy of combining STAT3 downregulation with anti-PD-1, we treated Treg cells with Stattic after anti-PD-1 treatment for 48 hours *in vitro* (Figure 4J-K). To our expectations, the STAT3 downregulation with anti-PD-1 therapy-induced to decreased expression of Tim-3 on Treg cells (Figure 4J). The immunosuppressive cytokines of TGF- β were also analyzed in Treg cells (Figure 4K). A slight decrease of TGF- β production was found in Treg cells with PD-1 and STAT3 pathways blockade (Figure 4K). Altogether, these findings confirmed that targeting STAT3 could abrogate the immunosuppression of Treg cells, providing a potential target in melanoma treatment.

STAT3 inhibitor enhances the efficacy of anti-PD-1 in melanoma

For the identification part of Tim-3 expression on tumor expansion, we established an immunocompetent that had been found for the skin melanoma model using B16-F10 cells. The generated melanoma mouse models were obtained with four different treatments: IgG for control, a PD-1 antibody, Stattic, and anti-PD-1 combination with Stattic (Figure 5A). First, we found that mice bodyweight in the anti-PD-1 treatment group was increased during the tumor progression, while STAT3 downregulated did not alter mice's weight (Figure 5B). Expectedly, in the PD-1 blockade group, anti-PD-1 treatment did not alter the tumor growth in the melanoma model (Figure 5C). Interestingly, in the combination group, we also found a marked reduction in tumor growth in the B16-F10 melanoma mouse model (Figure 5D, $p < 0.0001$). Under these conditions, STAT3 downregulation significantly increased the anti-PD-1 efficacy in melanoma. *In vivo* depletion experiments also demonstrated that the STAT3 pathway blockaded were essential in inhibiting tumor progression, suggesting a potential target therapy.

To confirm the efficacy of combining STAT3 blockade with anti-PD-1 in the C57BL/6 animal model, we performed H&E and TUNEL staining of tumors. Tumor metastasis and apoptosis were evaluated by H&E and TUNEL staining experiments. A significant increase for tumor cell necrosis on melanoma was observed in the STAT3 inhibitor group with anti-PD-1 therapy, indicating excellent therapy efficacy (Figure 5E). Moreover, H&E staining showed no evident metastasis of spleens in the Stattic and anti-PD-1 co-treatment group (Figure 5E). TUNEL staining results confirmed that the frequency of apoptosis cells was increased after STAT3 depletion with blockade (Figure 5E). Therefore, these data suggest that Stattic with PD-1 blockade inhibits tumor growth and metastasis, providing potential therapy for melanoma treatment.

To determine the impact of STAT3 downregulation on anti-melanoma immune response, we analyzed the cell phenotype and cytokine expression pattern in spleen tissue using flow cytometry (Figure 5F). We found a gradient of low down to elevated degrees of immune cells in the spleen (Figure 5F). As expected, the flow cytometric study elaborates that CD4⁺ and CD8⁺ T cells had been exceedingly concentrated within the cell clusters (Figure 5F). Next, we explored CD8⁺ T cell-driven cytokines and multi-inhibitory receptors for disclosing the fundamental downstream mechanisms. Analysis of CD8 subsets, assessed by the manifestation of PD-1, Tim-3, IL-10, TGF- β , granzyme B, and the levels of p-STAT3, indicated that Tim-3 and TGF- β were differentially expressed in these subsets with a distinct transcriptional signature compared to that of other subsets (Figure 5G). These results suggest a potential mechanism of Tim-3 regulation in anti-melanoma immunity.

Blockade STAT3 pathway promotes anti-melanoma immune response

To examine the influence of STAT3 downregulation upon the anti-tumor immune response, we analyzed the tumor infiltrated lymphocytes that had been studied in melanoma mice. Interestingly, STAT3 depletion and anti-PD-1 therapy decreased the percentages of CD8⁺ and CD4⁺T cells, leading to an increased CD8/CD4 ratio in STAT3 downregulation and PD-1 blockade combinational treatment in melanoma

according for monitoring mice or PD-1 blockade group (Figure 6A-C). Similar results were observed in STAT3 downregulation when compared to the control group (Figure 6B-C). Moreover, *in vivo* experiments confirmed a marked reduction in the percentages of Treg cells upon to STAT3 inhibitor with anti-PD-1 antibody (Figure 6D). The findings implied that Treg cells were essential in the inhibition of tumor growth (Figure 6D, $p < 0.05$). To understand how the STAT3 pathway regulates the tumor infiltrated Treg cells, we evaluated the expression of Tim-3 and immunosuppressive cytokines. Our data identified that the PD-1 pathway blockade upregulated the proportion of Tim-3 expression on melanoma-associated Treg cells (Figure 6E). While combining STAT3 downregulation and anti-PD-1 decreased the manifestation of Tim-3 on Treg cells during the anti-tumor response (Figure 6E). Moreover, we observed a slight rise in the secretion of TGF- β and IL-10 in the anti-PD-1 group compared to the IgG2a group (Figure 6F-G), which was similar to *in vitro* data. Furthermore, flow cytometric analysis demonstrated that STAT3 inhibitor with PD-1 treatment weakened the secretion of TGF- β and IL-10 on Treg cells compared to anti-PD-1 treatment melanoma mice, implying an enhanced anti-tumor immunity (Figure 6 F-G). These data suggested combination therapy with anti-PD-1 and STAT3 pathway inhibitor could promote the anti-tumor immunity and suppressed the tumor progression. Thus, the above data suggested that Tim-3 expression on Treg cells in the TME is STAT3-dependent, providing further support for STAT3 as a target and enhancing the immunotherapy for patients suffering from melanoma.

To confirm the role of combination STAT3 downregulation and anti-PD-1 treatment on CD8⁺ T cells, we analyzed the cell phenotype and cytokine expression pattern of CD8⁺ T cells in melanoma (Figure S3A-C). Interestingly, there was a reverse trend in CD8 T cells compared with Treg cells after different treatments (Figure S3A-C). STAT3 downregulation with and without anti-PD-1 therapy was related to an increased expression of Tim-3 on CD8⁺ T cells as an activation towards CD8⁺T cells (Figure S3A). Moreover, the STAT3 blockade induced secretion of IL-10 and TGF- β in CD8⁺ T cells compared that in IgG-treated mice (Figure S3B-C). Our finding indicated that STAT3 presents a reverse event in the crosstalk between Treg cells and CD8⁺ T cells. Altogether, these results strongly identified that STAT3 downregulation damped Treg function in melanoma, enhanced the anti-tumor immunity. Based on the above data, our work demonstrates that Tim-3 was upregulated through the STAT3 pathway in checkpoint receptors inhibitor therapy.

Furthermore, to investigate the systemic toxicity after different treatments, we conducted the main organs of the H&E staining experiment, including the heart, liver, lungs, kidneys, and brains. There was no apparent toxicity in the main organs after the end of treatment (Figure 6H). Based on these data, our work raises safety therapy by combination using p-STAT3 inhibitor Stattic and anti-PD-1 to regulate tumor immune therapy.

Discussion

Our study provides evidence that the STAT3 pathway behaves as an immune mediator, increasing Tim-3 expression in the TME and affecting the response to anti-PD-1 treatment in melanoma. Recently, Tim-3

has been identified within presenting the core part within effector T cells and cytokine fabrication within peripheral and TILs [25, 26]. In human patients with melanoma, high Tim-3 expressions are linked with the tiredness of tumor-infiltrating CD8⁺ T cells, and Tim-3 monoclonal antibodies reverse tumor-induced T cell exhaustion [27, 28]. However, Tim-3 is not usually voiced on Treg cells, except on those in a TME upon stimulation of tumor-associated antigens [29]. A study showed that almost 60% of tumor-infiltrating Treg cells in diseased persons having lung cancer expressed Tim-3, promoting tumor suppression [30]. Tim-3⁺ Treg cells were found to present much more tumor immunosuppression than Tim-3⁻ Treg cells in lung cancer patients, with the secretion of IL-10 and granzymes [31]. Compared with Tim-3⁻ Treg cells, Tim-3⁺ Treg cells presented high suppressive capacity by inhibiting the proliferation of conventional T cells [32]. Tim-3⁺ has been demonstrated as a marker of Treg cells in immunosuppression, dampening the effector function of CD8⁺ T cells [33]. Tim-3⁺ TIL Treg cell was much more suppressive than PD-1 higher expression Treg cells, which were known as exhausted Treg cells [34]. Moreover, Tim-3 overexpression has been identified in various diseases, including head and neck cancer, and bladder cancer [35–37]. High Tim-3 expression is related to poor survival of patients with many types of tumors in a clinical study [38]. However, its role in Treg cells on melanoma has not been described. Interestingly, the obtained results suggested that a low response to PD-1/PD-L1 in lung cancer patients is associated with higher Tim-3 expression [39]. The previous study identified that effective PD-1 blockade decreased Tim-3 expression on Treg cells in HNSCC tumors [16]. While the dynamic changes of Tim-3 on Treg cells in anti-PD-1 nonresponse melanoma patients have not been elucidated. Herein, we demonstrated that the upregulation of Tim-3 on Treg cells correlated with anti-PD-1 resistance melanoma patients. Notably, the proportion of Tim-3 expression on Treg cells upregulated after the PD-1 blockade in a murine melanoma model. *In vitro*, we also observed an increased production of suppressive factors (TGF-β) after anti-PD-1 therapy, which was related to the upregulation of Tim-3 expression on Treg cells. These results highlighted those Tim-3 expressions on Treg cells induced tumor immunosuppression in the TME. Our study also provides a potent combination of immune checkpoints receptors to enhance the therapeutic response using PD-1 and Tim-3 antibodies in cancer.

STAT3 is a member of the signal transduction and activator of transcription family mediating tumor proliferation, progression, metastasis, and immunity in the tumor microenvironment [40]. The JAK-STAT signaling pathway regulated the transcription of DNA and expression of genes involved in cancer behavior: tumor apoptosis and tumor angiogenesis [41, 42]. Evidence has demonstrated that the JAK/STAT3 pathway mediated tumor angiogenesis by increasing expression and activation of environmental hypoxia in TME [43]. Therefore, inhibiting STAT3 pathways can significantly reduce vascular endothelial growth factors, which could inhibit tumor growth. Our work indicated that the downregulation of STAT3 decreased melanoma growth in the murine mouse model. It is unlikely to deny the potential impact of STAT3 downregulation on tumor angiogenesis inhibition.

Herein, results have demonstrated that STAT3 downregulation in melanoma markedly reduced the proportion of tumor infiltrated Treg cells. Although the role of Treg cells in immunosuppression has been well illustrated, the activities of Treg cells under the PD-1 blockade are still unknown. Indeed, this study

demonstrated the role of STAT3 in the modulation of tumor infiltrated Treg cells *in vitro* and *in vivo* melanoma mouse models. The STAT3 pathway has been found to act as a co-transcription pathway for Foxp3 and to mediate other associated STAT3 targets, including IL-10, in Treg cells [19]. Previous studies have shown that STAT3 expression in Treg cells is associated with a suppressive function [21]. To explore the crucial role of Treg cells, we conducted a flow analysis of TILs composition. Treg cells in the B16F10 melanoma tumor model showed increased infiltration after anti-PD-1 while in a low CD8/CD4 ratio, suggesting immune escape in checkpoint blockade. Besides, our results demonstrated that p-STAT3 in Treg cells upregulated with increasing TGF- β production in animal models of melanoma after the PD-1 pathway blockade. Thus, these data confirmed that STAT3 expression is upregulated to adaptive resistance to PD-1 blockade in Treg cells in TME. These data highlighted the essential role of STAT3 in the regulation of melanoma immune escape. Thereby, blockaded the STAT3 pathway can be an excellent target to promote immunotherapy response. Treg cells can induce immunosuppression by secreting the molecules TGF- β via contact-dependent or contact-independent mechanisms [16, 44]. TGF- β is synthesized and secreted within the cells and promotes Treg cell development [45, 46]. To understand the molecular mechanisms of Treg upon anti-PD-1 therapy, we analyzed the production of immunosuppressive factors on Treg cells, such as TGF- β . We observed that purified Treg cells exhibited increased production of TGF- β after PD-1 blockade *in vitro*; these molecules presented an essential role in tumor immune escape. Moreover, TGF- β was found to markedly reduced by STAT3 depletion, resulting in a decrease of Treg cells. Further studies on the role and mechanism of TGF- β on Treg cells are regulated by the STAT3 pathway needed to explore in the future.

However, the molecular mechanism through which Tim-3 levels on Treg cells mediate by anti-PD-1 therapy remains unclear. Literature has demonstrated that Tim-3 expression is associated with STAT3 expression and phosphorylation in immunosuppression [10]. Herein, this work provides evidence that the upregulation of Tim-3 played a crucial role in anti-PD-1 resistance melanoma patients. To explore whether the immune checkpoint expression of Tim-3 changes through STAT3 pathways, we analyzed the expression and correlations of these genes. The examination of the TCGA data, IHC results, and melanoma gene profiles in our study demonstrated a strong relationship among Tim-3 (HAVCR2), PD1 (PDCD1), and STAT3 expression. These findings identified the vital role of STAT3 in the expression of Tim-3. Thus, inhibiting STAT3 may demonstrate an excellent activity on the downregulation of Tim-3, increasing the immune activities in melanoma. We further assessed the dynamic expression of Tim-3 on Treg cells to confirm the regulation of STAT3 after Static therapy. Expression of Tim-3 decreased with PD-1 upregulation on Treg cells after the STAT3 pathway blockade *in vitro*. These data suggested that the STAT3 pathway mediated the expression of Tim-3 on Treg cells in melanoma. According to the above results, we hypothesized that Tim-3 was upregulated through the STAT3 pathway after the PD-1 blockade to decrease the anti-PD-1 response. In melanoma models, the expression of Tim-3 on Treg cells decreased, but there was no significant change in Static-treated mice compared with the control mice. These data confirmed that Tim-3 was mediated by stimulating TCR signaling to STAT3 pathways during PD-1 blockade (Fig. 7). But it remains to be explored in the future whether STAT3 inhibitors act directly on Treg cells, which subsequently modulate the TME through tumor-associated antigens. As presented here,

the combination of a STAT3 inhibitor and anti-PD-1 identified significantly benefit of synthesis therapy. The results from the C57BL/6 tumor samples showed that STAT3 targeting combined with PD-1 blockade leads to a high CD8/CD4 ratio, a decreased percentage of Treg cells. Although the combination therapy presented excellent anti-tumor immunity, the efficacy of other cancer models has not been identified. The information reinforced that Tim-3 was mediated by stimulating TCR signaling to STAT3 pathways during PD-1 blockade in melanoma, providing further support for combination STAT3 inhibitor and anti-PD-1 therapy for patients suffering from melanoma. But it remains to be explored in the future whether STAT3 inhibitors act directly on Treg cells, which consequently alter the TME through tumor-associated antigens.

Conclusions

Finally, our current work addressed that Tim-3 presented the key character within Treg cells in anti-PD-1 resistance of melanoma. In this study, we reveal a potential mechanism by the STAT3 pathway, which regulated Tim-3 manifestation upon Treg cells in the immune microenvironment. Targeting Treg cells with the STAT3 inhibitor Stattic decreases Tim-3 articulation mutually *in vitro* and *in vivo*, increasing the immunotherapy efficacy by anti-PD-1. Further observations and experiments should be performed to address the mechanism of patient responses to combination therapies in melanoma. Moreover, the potential immunotherapy effect of combination STAT3 antagonists with other checkpoint receptor inhibitors and other immune cells like $\gamma\delta$ Treg cells and M2 macrophages involving in synthetic therapy are needed to explore. In summary, our work supports that Tim-3 expression modulated the immune escape in melanoma as a biomarker for predicting the immunotherapy response. Also, we identified that the transient small-molecule reticence of the STAT3 pathway may dramatically expand the usefulness of anti-PD-1 within melanoma. Therefore, our work provides a potential therapy for STAT3 as a target in melanoma treatment, supporting combining anti-PD-1 and STAT3 antagonists as excellent therapy.

Abbreviations

PD-1

Programmed cell death-1

TME

Tumor Microenvironment

Tim-3

T cell immunoglobulin and mucin-domain containing-3

Treg

Regulatory T

HNSCC

Head and Neck squamous cell

TILs

Tumor-infiltrating Lymphocytes

STAT3

Signal transduction and activator of transcription 3

Foxp3

Forkhead box P3

IL-10

Interleukin-10

TGF- β

transforming growth factor

ATCC

American Type Culture Collection

DMEM

Dulbecco's Modified Eagle Medium

FBS

Fetal Bovine Serum

IHC

Immunohistochemistry

PBMCs

Peripheral blood mononuclear cells

H&E

Haematoxylin and Eosin

TUNEL

dUTP-biotin nick end labeling assay

TCGA

The Cancer Genome Atlas

RNA-seq

RNA sequencing

Declarations

Availability of data and materials

All data generated or analyzed during this study are available from the corresponding author upon reasonable request.

Ethics approval and consent to participate

All human specimens research protocol was reviewed and approved by the Ethics Committee of Shanghai Tenth People's Hospital (2019K39). Informed consent was obtained from all participants included in the study in agreement with institutional guidelines. All animal experiments were performed according to protocols and under the guidelines approved by the institutional Animal Care and Use Committee of Tongji University.

Consent for publication

All authors agree to submit the article for publication.

Availability of data and materials

The datasets used and/or analysed during the current study are available from the corresponding author on reasonable request.

Competing interests

The authors declare that they have no competing interests.

Funding

This work was supported by grants from the Shanghai Sailing Program (NO: 19YF1438300), Pujiang Fostering Program of Shanghai Tenth Peoples' Hospital (NO: 040118024), National Natural Science Fostering Foundation of Shanghai Tenth Peoples' Hospital (NO: DS040317061), Industry-university-research-medicine Project of Shanghai Science and Technology Commission (NO: 18DZ1910102) and National Natural Science Foundation of China (NO: 81702311, 81803090 and 81902896).

Author's contributions

LH performed and analyzed the animal examination and a major contributor in writing the manuscript. YX analyzed the interpreted the patient data regarding the immunity of melanoma. JF performed the histological examination of the tumor samples and other organs. WL acquired and analyzed the flow data and reviewed the manuscript. ZL and LH developed the methodology of this study. JC, ZL, and QX conducted the conception and design of the manuscript. All authors read and approved the final manuscript.

Acknowledgments

We thank the supports of shanghai power hospital.

References

1. Topalian SL, Taube JM, Anders RA, Pardoll DM. Mechanism-driven biomarkers to guide immune checkpoint blockade in cancer therapy. *Nat Rev Cancer*. 2016;16(5):275-287.
2. Brahmer JR, Tykodi SS, Chow LQ, Hwu WJ, Topalian SL, Hwu P, Drake CG, Camacho LH, Kauh J, Odunsi K et al. Safety and activity of anti-PD-L1 antibody in patients with advanced cancer. *N Engl J Med*. 2012;366(26):2455-2465.
3. Bellmunt J, Powles T, Vogelzang NJ. A review on the evolution of PD-1/PD-L1 immunotherapy for bladder cancer: The future is now. *Cancer Treat Rev*. 2017;54:58-67.
4. Robert C, Long GV, Brady B, Dutriaux C, Maio M, Mortier L, Hassel JC, Rutkowski P, McNeil C, Kalinka-Warzocha E et al. Nivolumab in previously untreated melanoma without BRAF mutation. *N Engl J*

- Med. 2015;372(4):320-330.
5. Gibney GT, Kudchadkar RR, DeConti RC, Thebeau MS, Czupryn MP, Tetteh L, Eysmans C, Richards A, Schell MJ, Fisher KJ et al. Safety, correlative markers, and clinical results of adjuvant nivolumab in combination with vaccine in resected high-risk metastatic melanoma. *Clin Cancer Res.* 2015;21(4):712-720.
 6. Melero I, Berman DM, Aznar MA, Korman AJ, Perez Gracia JL, Haanen J. Evolving synergistic combinations of targeted immunotherapies to combat cancer. *Nat Rev Cancer.* 2015;15(8):457-472.
 7. Liu Y, Cai P, Wang N, Zhang Q, Chen F, Shi L, Zhang Y, Wang L, Hu L. Combined blockade of Tim-3 and MEK inhibitor enhances the efficacy against melanoma. *Biochem Biophys Res Commun.* 2017;484(2):378-384.
 8. Wherry EJ, Kurachi M. Molecular and cellular insights into T cell exhaustion. *Nat Rev Immunol.* 2015;15(8):486-499.
 9. Fourcade J, Sun Z, Benallaoua M, Guillaume P, Luescher IF, Sander C, Kirkwood JM, Kuchroo V, Zarour HM. Upregulation of Tim-3 and PD-1 expression is associated with tumor antigen-specific CD8+ T cell dysfunction in melanoma patients. *J Exp Med.* 2010;207(10):2175-2186.
 10. Gautron AS, Dominguez-Villar M, de Marcken M, Hafler DA. Enhanced suppressor function of TIM-3+ FoxP3+ regulatory T cells. *Eur J Immunol.* 2014;44(9):2703-2711.
 11. Gupta S, Thornley TB, Gao W, Larocca R, Turka LA, Kuchroo VK, Strom TB. Allograft rejection is restrained by short-lived TIM-3+PD-1+Foxp3+ Tregs. *J Clin Invest.* 2012;122(7):2395-2404.
 12. Das M, Zhu C, Kuchroo VK. Tim-3 and its role in regulating anti-tumor immunity. *Immunol Rev.* 2017;276(1):97-111.
 13. Kageshita T, Kashio Y, Yamauchi A, Seki M, Abedin MJ, Nishi N, Shoji H, Nakamura T, Ono T, Hirashima M. Possible role of galectin-9 in cell aggregation and apoptosis of human melanoma cell lines and its clinical significance. *Int J Cancer.* 2002;99(6):809-816.
 14. Penalzoza-MacMaster P, Kamphorst AO, Wieland A, Araki K, Iyer SS, West EE, O'Mara L, Yang S, Konieczny BT, Sharpe AH et al. Interplay between regulatory T cells and PD-1 in modulating T cell exhaustion and viral control during chronic LCMV infection. *J Exp Med.* 2014;211(9):1905-1918.
 15. Rallon N, Garcia M, Garcia-Samaniego J, Cabello A, Alvarez B, Restrepo C, Nistal S, Gorgolas M, Benito JM. Expression of PD-1 and Tim-3 markers of T-cell exhaustion is associated with CD4 dynamics during the course of untreated and treated HIV infection. *PLoS One.* 2018;13(3):e0193829.
 16. Liu Z, McMichael EL, Shayan G, Li J, Chen K, Srivastava R, Kane LP, Lu B, Ferris RL. Novel Effector Phenotype of Tim-3(+) Regulatory T Cells Leads to Enhanced Suppressive Function in Head and Neck Cancer Patients. *Clin Cancer Res.* 2018;24(18):4529-4538.
 17. Wang Y, Shen Y, Wang S, Shen Q, Zhou X. The role of STAT3 in leading the crosstalk between human cancers and the immune system. *Cancer Lett.* 2018;415:117-128.
 18. Lee JS, Kang JH, Boo HJ, Hwang SJ, Hong S, Lee SC, Park YJ, Chung TM, Youn H, Mi Lee S et al. STAT3-mediated IGF-2 secretion in the tumour microenvironment elicits innate resistance to anti-IGF-1R antibody. *Nat Commun.* 2015;6:8499.

19. Hossain DM, Panda AK, Manna A, Mohanty S, Bhattacharjee P, Bhattacharyya S, Saha T, Chakraborty S, Kar RK, Das T et al. FoxP3 acts as a cotranscription factor with STAT3 in tumor-induced regulatory T cells. *Immunity*. 2013;39(6):1057-1069.
20. Oweida AJ, Darragh L, Phan A, Binder D, Bhatia S, Mueller A, Van Court B, Milner D, Raben D, Woessner R et al. STAT3 Modulation of Regulatory T Cells in Response to Radiation Therapy in Head and Neck Cancer. *J Natl Cancer Inst*. 2019;
21. Yang L, Li B, Dang E, Jin L, Fan X, Wang G. Impaired function of regulatory T cells in patients with psoriasis is mediated by phosphorylation of STAT3. *J Dermatol Sci*. 2016;81(2):85-92.
22. Zorn E, Nelson EA, Mohseni M, Porcheray F, Kim H, Litsa D, Bellucci R, Raderschall E, Canning C, Soiffer RJ et al. IL-2 regulates FOXP3 expression in human CD4+CD25+ regulatory T cells through a STAT-dependent mechanism and induces the expansion of these cells in vivo. *Blood*. 2006;108(5):1571-1579.
23. Kong LY, Wei J, Sharma AK, Barr J, Abou-Ghazal MK, Fokt I, Weinberg J, Rao G, Grimm E, Priebe W et al. A novel phosphorylated STAT3 inhibitor enhances T cell cytotoxicity against melanoma through inhibition of regulatory T cells. *Cancer Immunol Immunother*. 2009;58(7):1023-1032.
24. Kinjyo I, Inoue H, Hamano S, Fukuyama S, Yoshimura T, Koga K, Takaki H, Himeno K, Takaesu G, Kobayashi T et al. Loss of SOCS3 in T helper cells resulted in reduced immune responses and hyperproduction of interleukin 10 and transforming growth factor-beta 1. *J Exp Med*. 2006;203(4):1021-1031.
25. Avery L, Filderman J, Szymczak-Workman AL, Kane LP. Tim-3 co-stimulation promotes short-lived effector T cells, restricts memory precursors, and is dispensable for T cell exhaustion. *Proc Natl Acad Sci U S A*. 2018;115(10):2455-2460.
26. Sabins NC, Chornoguz O, Leander K, Kaplan F, Carter R, Kinder M, Bachman K, Verona R, Shen S, Bhargava V et al. TIM-3 Engagement Promotes Effector Memory T Cell Differentiation of Human Antigen-Specific CD8 T Cells by Activating mTORC1. *J Immunol*. 2017;199(12):4091-4102.
27. Baitsch L, Baumgaertner P, Devereux E, Raghav SK, Legat A, Barba L, Wieckowski S, Bouzourene H, Deplancke B, Romero P et al. Exhaustion of tumor-specific CD8(+) T cells in metastases from melanoma patients. *J Clin Invest*. 2011;121(6):2350-2360.
28. da Silva IP, Gallois A, Jimenez-Baranda S, Khan S, Anderson AC, Kuchroo VK, Osman I, Bhardwaj N. Reversal of NK-cell exhaustion in advanced melanoma by Tim-3 blockade. *Cancer Immunol Res*. 2014;2(5):410-422.
29. Sasidharan Nair V, Elkord E. Immune checkpoint inhibitors in cancer therapy: a focus on T-regulatory cells. *Immunol Cell Biol*. 2018;96(1):21-33.
30. Gao X, Zhu Y, Li G, Huang H, Zhang G, Wang F, Sun J, Yang Q, Zhang X, Lu B. TIM-3 expression characterizes regulatory T cells in tumor tissues and is associated with lung cancer progression. *PLoS One*. 2012;7(2):e30676.
31. Monney L, Sabatos CA, Gaglia JL, Ryu A, Waldner H, Chernova T, Manning S, Greenfield EA, Coyle AJ, Sobel RA et al. Th1-specific cell surface protein Tim-3 regulates macrophage activation and severity

- of an autoimmune disease. *Nature*. 2002;415(6871):536-541.
32. Zhang HF, Liang GB, Zhao MG, Zhao GF, Luo YH. Regulatory T cells demonstrate significantly increased functions following stimulation with IL-2 in a Tim-3-dependent manner in intracranial aneurysms. *Int Immunopharmacol*. 2018;65342-347.
 33. Yan J, Zhang Y, Zhang JP, Liang J, Li L, Zheng L. Tim-3 expression defines regulatory T cells in human tumors. *PLoS One*. 2013;8(3):e58006.
 34. Lowther DE, Goods BA, Lucca LE, Lerner BA, Raddassi K, van Dijk D, Hernandez AL, Duan X, Gunel M, Coric V et al. PD-1 marks dysfunctional regulatory T cells in malignant gliomas. *JCI Insight*. 2016;1(5):
 35. Li F, Li N, Sang J, Fan X, Deng H, Zhang X, Han Q, Lv Y, Liu Z. Highly elevated soluble Tim-3 levels correlate with increased hepatocellular carcinoma risk and poor survival of hepatocellular carcinoma patients in chronic hepatitis B virus infection. *Cancer Manag Res*. 2018;10941-951.
 36. Yang M, Yu Q, Liu J, Fu W, Cao Y, Yu L, Shao S, Wang X, Niu H, Wang Y. T-cell immunoglobulin mucin-3 expression in bladder urothelial carcinoma: Clinicopathologic correlations and association with survival. *J Surg Oncol*. 2015;112(4):430-435.
 37. Shayan G, Srivastava R, Li J, Schmitt N, Kane LP, Ferris RL. Adaptive resistance to anti-PD1 therapy by Tim-3 upregulation is mediated by the PI3K-Akt pathway in head and neck cancer. *Oncoimmunology*. 2017;6(1):e1261779.
 38. Li H, Wu K, Tao K, Chen L, Zheng Q, Lu X, Liu J, Shi L, Liu C, Wang G et al. Tim-3/galectin-9 signaling pathway mediates T-cell dysfunction and predicts poor prognosis in patients with hepatitis B virus-associated hepatocellular carcinoma. *Hepatology*. 2012;56(4):1342-1351.
 39. Koyama S, Akbay EA, Li YY, Herter-Sprie GS, Buczkowski KA, Richards WG, Gandhi L, Redig AJ, Rodig SJ, Asahina H et al. Adaptive resistance to therapeutic PD-1 blockade is associated with upregulation of alternative immune checkpoints. *Nat Commun*. 2016;710501.
 40. Avalle L, Camporeale A, Camperi A, Poli V. STAT3 in cancer: A double edged sword. *Cytokine*. 2017;9842-50.
 41. Groner B, von Manstein V. Jak Stat signaling and cancer: Opportunities, benefits and side effects of targeted inhibition. *Mol Cell Endocrinol*. 2017;4511-14.
 42. Liu JF, Deng WW, Chen L, Li YC, Wu L, Ma SR, Zhang WF, Bu LL, Sun ZJ. Inhibition of JAK2/STAT3 reduces tumor-induced angiogenesis and myeloid-derived suppressor cells in head and neck cancer. *Mol Carcinog*. 2018;57(3):429-439.
 43. Itsuji T, Tonomura H, Ishibashi H, Mikami Y, Nagae M, Takatori R, Tanida T, Matsuda KI, Tanaka M, Kubo T. Hepatocyte growth factor regulates HIF-1alpha-induced nucleus pulposus cell proliferation through MAPK-, PI3K/Akt-, and STAT3-mediated signaling. *J Orthop Res*. 2020;
 44. Halvorsen EC, Mahmoud SM, Bennewith KL. Emerging roles of regulatory T cells in tumour progression and metastasis. *Cancer Metastasis Rev*. 2014;33(4):1025-1041.
 45. ten Dijke P, Arthur HM. Extracellular control of TGFbeta signalling in vascular development and disease. *Nat Rev Mol Cell Biol*. 2007;8(11):857-869.

46. Maynard CL, Hatton RD, Helms WS, Oliver JR, Stephensen CB, Weaver CT. Contrasting roles for all-trans retinoic acid in TGF-beta-mediated induction of Foxp3 and Il10 genes in developing regulatory T cells. J Exp Med. 2009;206(2):343-357.

Tables

Table 1 Clinical and pathological features of puncture melanoma patients in this study

Gender	Age (at diagnosis)	Primary Tumor Site	TNM Stage	Puncture Site
Female	59	Nose	IV	Cervical lymph node
Female	55	Left Plantar	IV	Chest Wall
Male	76	Right Heel	IV	Lung
Female	49	Eye	IV	Liver
Male	48	Right Heel	III	Inguinal lymph node
Male	53	Upper limb	IV	Cervical lymph node

Figures

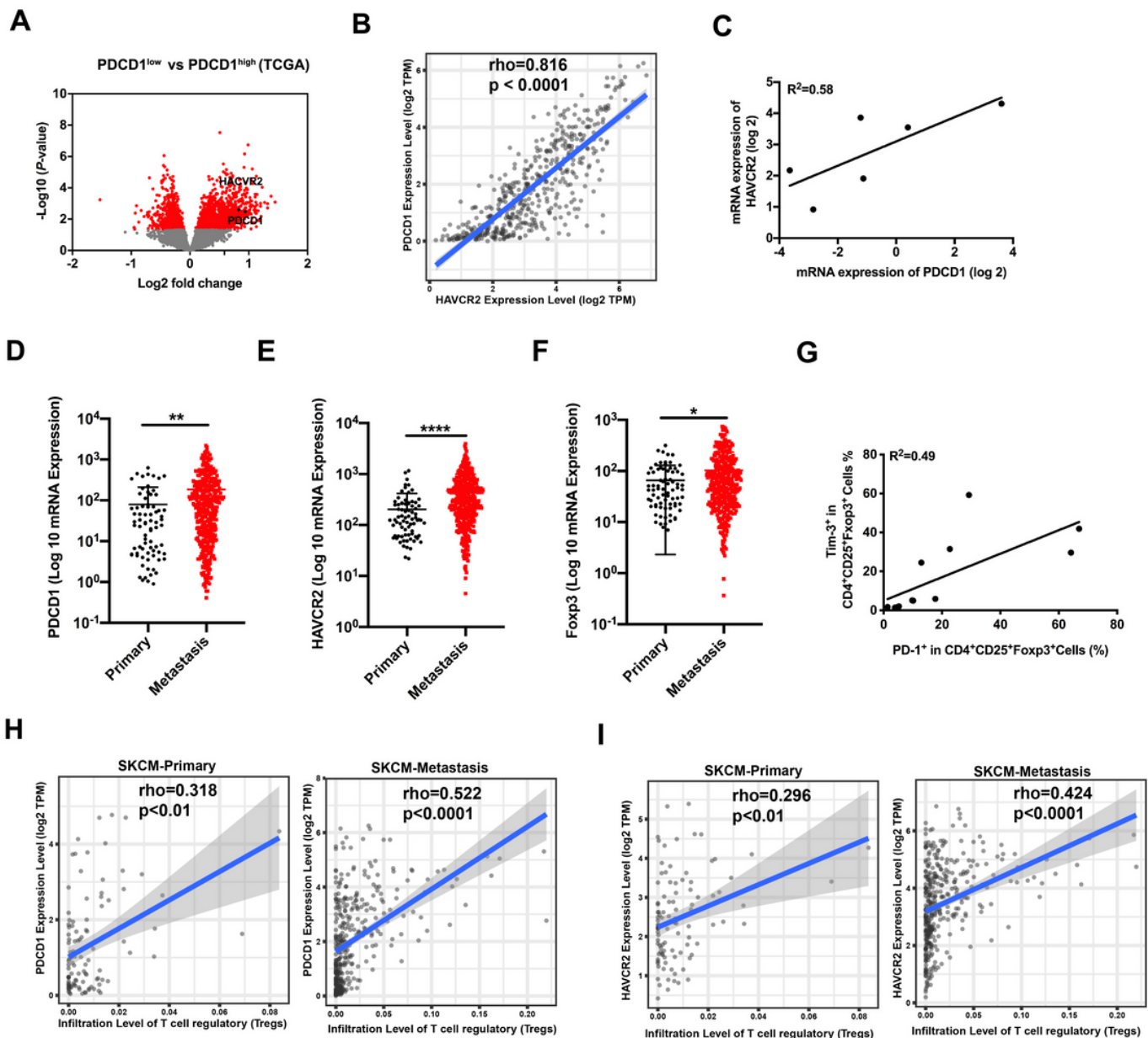


Figure 1

Correlation of PDCD1 expression and HAVCR2 in melanoma. a Volcano plot showing enrichment of differentially expressed genes in the PD-1^{high} and PD-1^{low} sub-populations from the TCGA dataset (n=472). Significantly different genes (PDCD1 and HAVCR2) are plotted in black (log₂ fold change > 0.5, p < 0.05). b Correlation between PDCD1 (PD-1) and HAVCR2 (Tim-3) expression in human melanoma samples from the TCGA dataset (n=472). c Association between the mRNA level of PDCD1 (PD-1) and HAVCR2 (Tim-3) from melanoma biopsies Pearson correlation of (n=6; R² values by linear regression). d-f PDCD1 (d), HAVCR2 (e), and Foxp3 (f) expression in primary and metastatic melanoma patients from the TCGA dataset. g Relationship of PD-1 and Tim-3 expression on Treg cells in PBMCs from healthy donors

(n=9; R2 values by linear regression). h-i Correlation between PDCD1 (h) or HAVCR2 (i) expression and Treg cells infiltration in primary and metastasis melanoma patients' samples from the TCGA datasets.

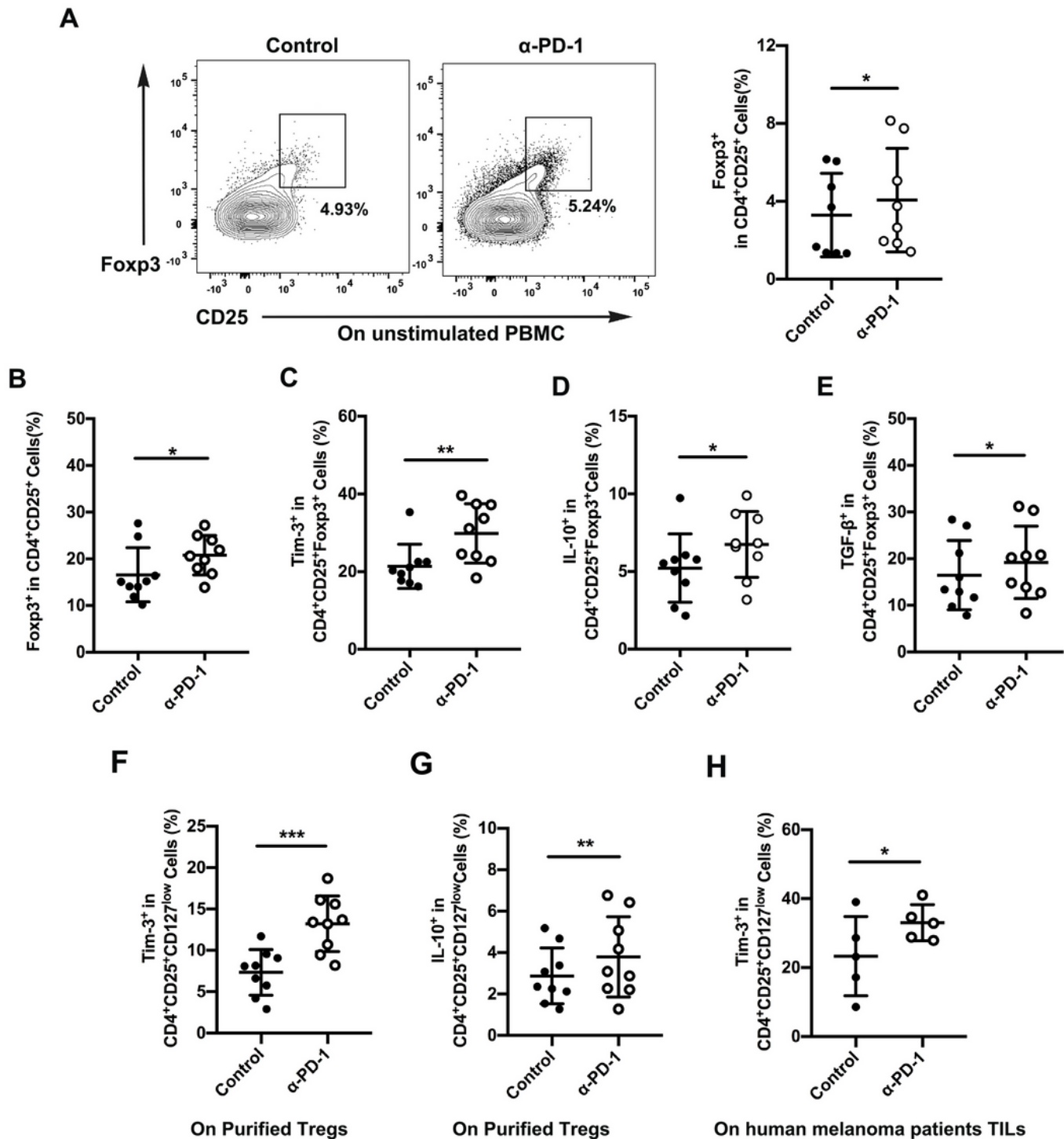
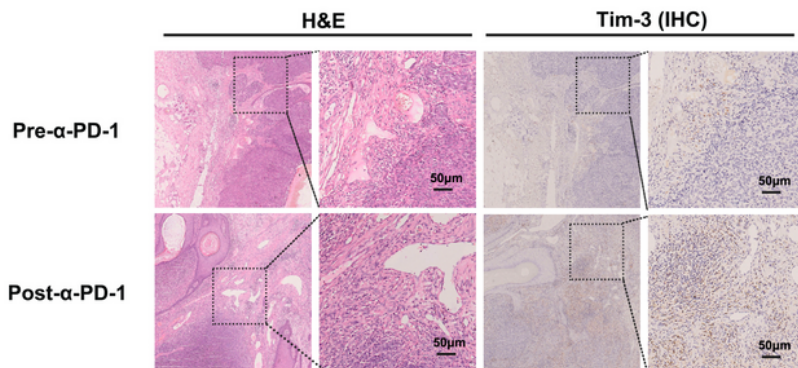


Figure 2

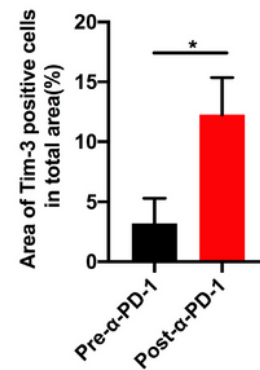
Tim-3 expression upregulated after PD-1 blockade on Treg cells. a-b Anti-PD-1 antibody (α -PD-1) was given at a concentration of $10 \mu\text{g mL}^{-1}$ in vitro for 48 h. The proportion of Treg cells in unstimulated (a) or (b) stimulate PBMCs were analyzed (n=9; $p < 0.05$). c-e Tim-3 expression, IL-10 and TGF- β production

were investigated by flow cytometry. Representative Tim-3 expression (c), IL-10 (d) and TGF- β secretion (e) in Treg cells after stimulation with PD-1 blockade (n=9; p < 0.01; p < 0.05; p < 0.05). f-g Purified Treg were subjected to anti-PD-1 therapy for 48 hours. Representative plots representing Tim-3 expression (f) and IL-10 (g) in Treg cells (n=9; p < 0.001). H Freshly isolated tumour-infiltrating lymphocytes (TILs) from melanoma patients were treated with nivolumab 10 μ g mL⁻¹ for 48 h. Tumour-infiltrating Treg cells from melanoma patients were analysed for Tim-3 expression (n=5; p < 0.05). Significance was calculated with t-text. All data are presented as the means \pm SEM, * p < 0.05; ** p < 0.01; *** p < 0.001.

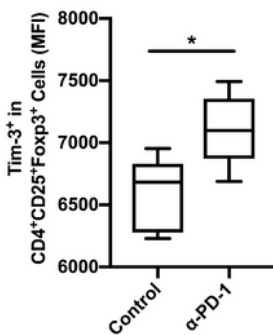
A



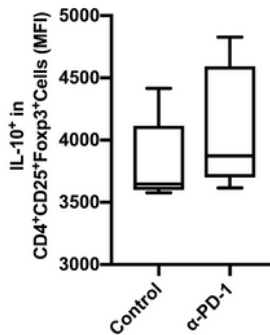
B



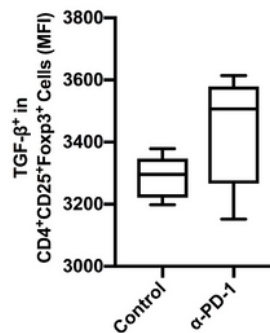
C



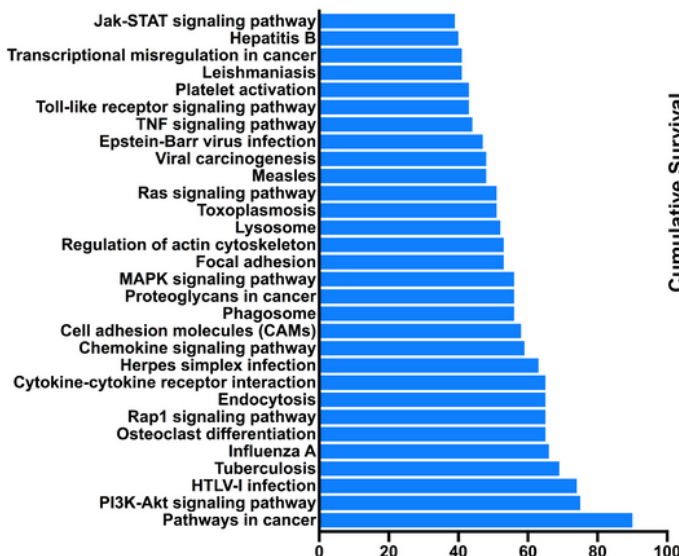
D



E



F



G

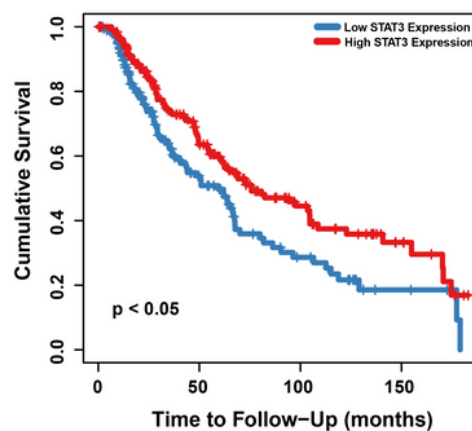


Figure 3

STAT3 pathway involved in PD-1 expression. a-b H&E and IHC for Tim-3 expression levels in anti-PD-1 resistance melanoma patients' tissue samples (n=3). Representative images from 3 patients displayed positive Tim-3 staining in stromal regions (a). Scale bar = 50 μ m. Quantification of positive cells in tumor sections using ImageJ software (b) Significance was calculated with a t-test, and all data are presented as the means \pm SEM. c-e Tim-3 expression(c), IL-10(d), and TGF- β (e) production in Treg cells were investigated by flow cytometry after anti-PD-1 treatment in the B16-F10 melanoma mouse model. f Significantly enriched pathways terms of differentially expressed genes in the PD-1^{high} and PD-1^{low} sub-populations in melanoma. The top 30 functional and signaling pathway enrichment were conducted using the online website of DAVID. g Overall survival of STAT3 expression associated with better relapse-free survival for melanoma patients.

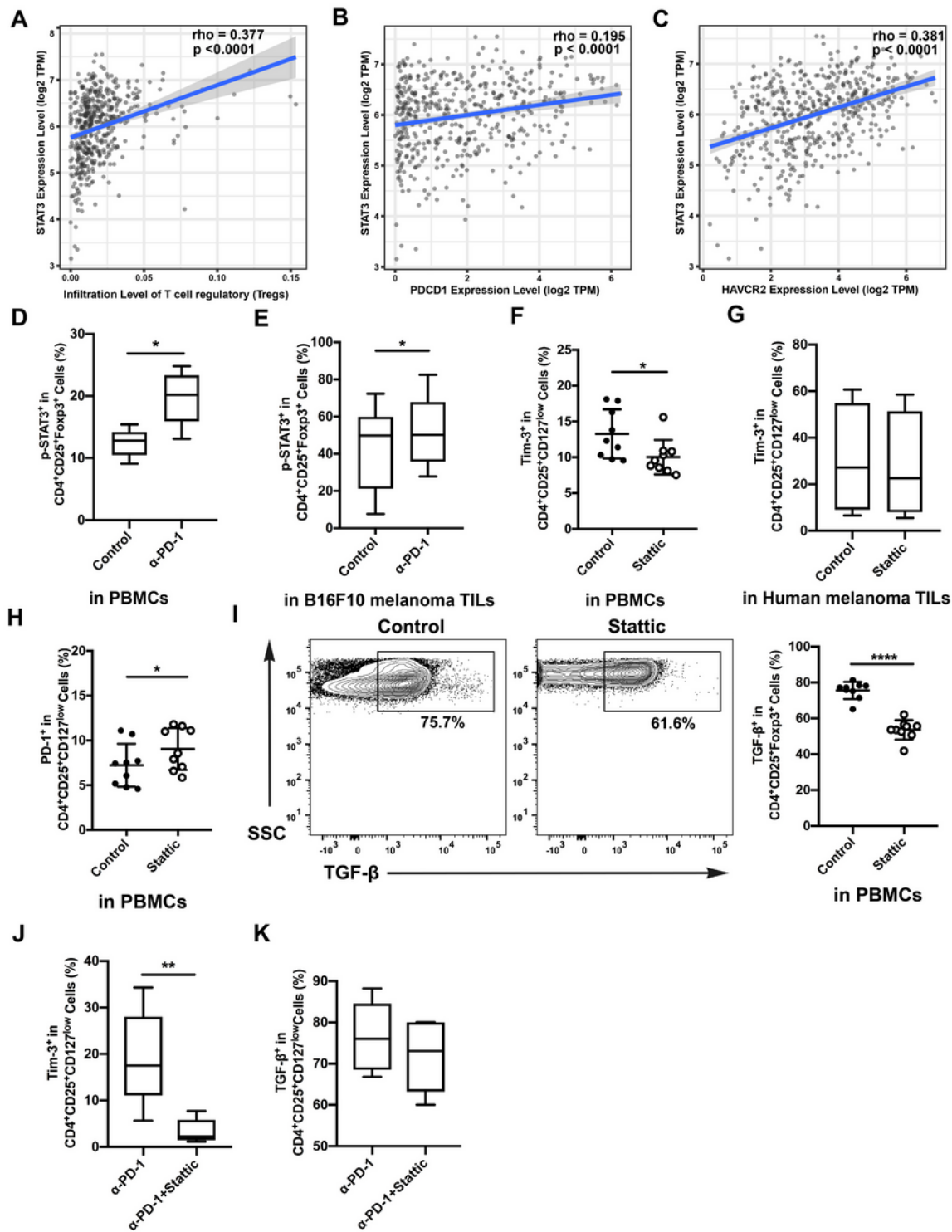


Figure 4

Relationship of STAT3 and Tim-3 in melanoma. a-c Correlation between STAT3 expression and tumor infiltrated Treg cells (a), the expressed genes PDCD1(b), and HAVCR2 (c) in human melanoma samples from the TCGA dataset. d-e p-STAT3 expression after anti-PD-1 treatment both in vitro (d) and in vivo (e). f-g Proportion of circulating Treg cells treated with STAT3 inhibitor compared to that of the control group. Analysis of the phenotypic expression of Tim-3 on Treg cells in PBMCs (f) and Human melanoma TILs

(g). h-i PD-1 expression (h) and TGF- β (i) production on Treg cells after the STAT3 pathway blockade were also analyzed. Significance was calculated with a t-test; all data are presented as the means \pm SEM, * $p < 0.05$ and ** $p < 0.01$. j-k Analysis of the expression of Tim-3 (j), and production of TGF- β (k) on purified Treg cells after anti-PD-1 treatment with Stattic. Significance was calculated with a t-test; all data are presented as the means \pm SEM, * $p < 0.05$ and ** $p < 0.01$.

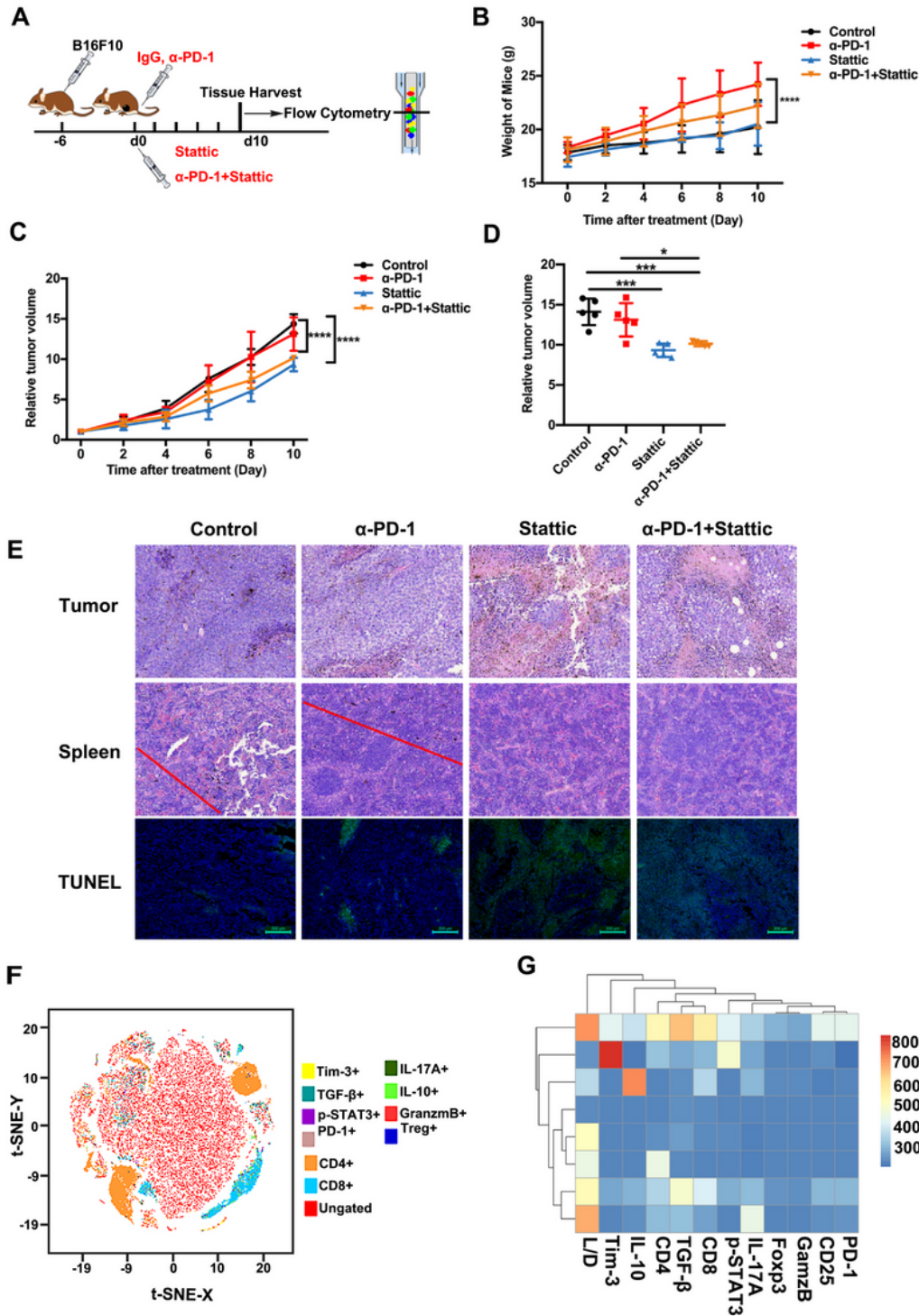


Figure 5

STAT3 inhibitor enhanced the efficacy of anti-PD-1 in a melanoma model. a Schematic illustration of different treatments in the melanoma mouse model. b Weight curve of B16-F10 tumors from mice administered different treatments (n=5; p <0.0001). c Relative tumor volume curve of B16-F10 tumors after treatment with anti-PD-1 alone, Stattic alone, anti-PD-1 plus Stattic, and IgG isotype control (n=5; p <0.0001). d Relative tumor volume at terminal time of experiments with four different treatments (n=5; p <0.05; p <0.001; p <0.001). e Tumour necrosis in tumor sections as indicated by hematoxylin and eosin (H&E) staining. Tumor metastasis to the spleen was assessed by H&E staining. Tumor apoptosis in tumor sections was examined using TUNEL staining. Scale bar = 50 μm or 100 μm . f tSNE plots of CD8+ T cells of spleen tissues from B16-F10 tumor-bearing mice. g Heat map of the tumor-associated gene signature mapped to the different tumor treatment, representing the spleen tissues and CD8+ T cells subsets from B16-F10 tumor-bearing mice.

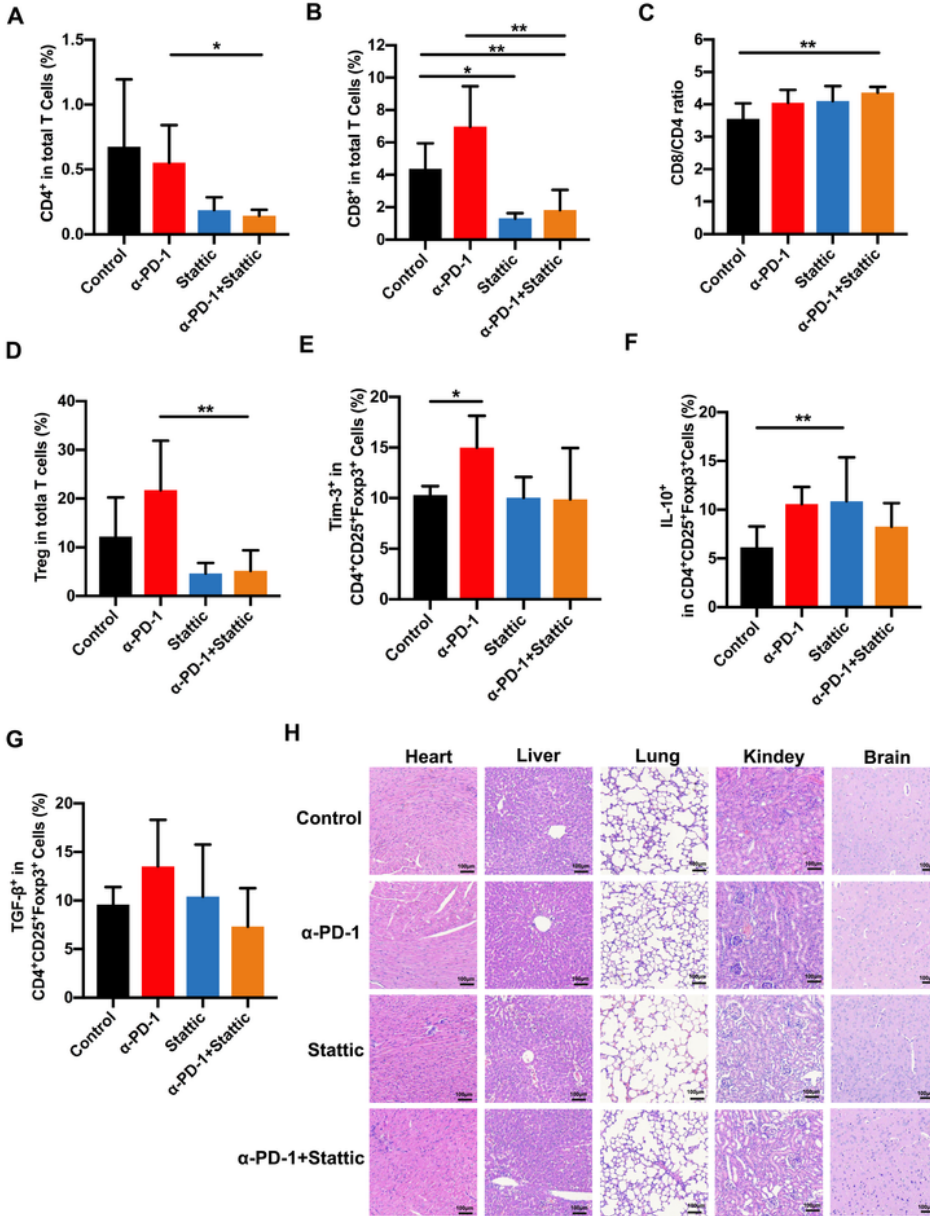


Figure 6

STAT3 downregulation promotes anti-tumor immune response. a-c Analysis of intratumoral CD4⁺ and CD8⁺ T cells in melanoma models. The proportion of intratumoral CD4 (a) cells and CD8 (b) T cells and CD8⁺/CD4⁺ T cells ratio (c) in response to anti-PD-1 in comparison to anti-PD-1 and Stattic, Stattic, and control groups. d Percentages of CD4⁺CD25⁺Foxp3⁺ Treg cells among total cells in melanoma (n=5). e-g percentage of positive Tim-3 expression (e), IL-10 (f), and TGF-β (g) production in Treg cells after different

treatment in a mouse model. h Systematic toxicity of anti-PD-1 and Sttatic in melanoma models. Organ was toxicity were assessed by H&E staining. Scale bar = 100 μ m.

Image not available with this version

Figure 7

Schematic illustration of the experimental design. Anti-PD-1 therapy-induced Tim-3 upregulation, IL-10, and TGF- β secretion through the STAT3 pathway in regulatory T cells in melanoma.

Supplementary Files

This is a list of supplementary files associated with this preprint. Click to download.

- [FigureS1.pdf](#)
- [FigureS1.pdf](#)
- [FigureS2.pdf](#)
- [FigureS2.pdf](#)
- [FigureS3.pdf](#)
- [FigureS3.pdf](#)